Proceedings of the XIII International Conference "Ion Implantation and Other Applications of Ions and Electrons"

Positron Beam Characteristics of Heavy Ion Irradiated Silver

P. Horodek* and K. Siemek

Institute of Nuclear Physics Polish Academy of Sciences, PL-31342 Krakow, Poland

Doi: 10.12693/APhysPolA.142.697 *e-mail: pawel.horodek@ifj.edu.pl

This paper reports experimental studies of silver after 167 MeV Xe^{26+} ions irradiation. Heavy ion implantation of samples with doses 2×10^{12}, 5×10^{12}, 10^{13}, 5×10^{13} and 10^{14} was performed at IC-100 cyclotron at FLNR, JINR. Radiation damages were investigated with variable energy positron beam. Doppler broadening spectroscopy was applied and the line shape S parameter of annihilation line was extracted. The analysis of S parameter profiles gives information about the presence of open volume defects in irradiated samples. The positron diffusion length extracted from the profile decreases with the dose increase. It points out the increase of defects concentration. Probably, changes in the size or type of defects generated by various doses took place.

topics: defects, silver, positron beam, irradiation, heavy ions

1. Introduction

Positron annihilation spectroscopy (PAS) is a suitable tool for detection irradiation-induced defects as vacancies, their clusters, dislocations etc. These are generated by different kinds of radiation such as neutron, electrons, gamma and ions and affect the implanted material properties, such as corrosion resistance, hardness, thermal conductivity, chemical composition or electric resistivity. For this reason, studies of irradiated materials are recently a popular direction of research. In this way, materials useful in the nuclear industry, such as alloys and oxides, are tested for their practical aspect. In turn, materials not popular in nuclear applications like pure metals, being the main composite of alloys such as iron, and with properties possible to reproduce in theoretical studies, are investigated for cognitive goals. Information about the concentration and kind of irradiation-induced defect can be obtained from PAS. This method allows one to detect damages with a concentration up to 10^{-7}, while in the case of commonly applied transmission electron microscopy (TEM), this threshold equals 10^{-3}. There is a well-known successful utilization of PAS in defect research [1–3]. The usage of low-energy monoenergetic positrons opens new perspectives for tracking damages at depths from single nanometers from the surface [4].

This paper reports positron beam studies of heavy ion irradiated pure silver. Due to the optical, electrical and mechanical properties, silver and its alloys have found application in manufacturing of jewellery, silver staining of glasses and in electronic technologies [5–6]. However, the number of studies conducted on pure silver is not rich and is incomparably smaller compared to other pure metals such as, e.g., iron or copper. In any case, Jenkins [7] observed vacancy clusters with a geometry based on a partially dissociated Frank loop and stacking-fault tetrahedra in silver exposed to 50 keV Ag ion implantation. Ahmad et al. [8] found strong antibacterial activity against both the Gram-positive and Gram-negative bacteria in irradiated silver and agar/silver nanoparticle samples. Due to this antibacterial activity, the authors pointed out new potentials for many applications, such as antibacterial food packaging and biomedical application of studied objects. Lauzier et al. [9] found that interstitials are stable on dislocations by testing the variation of Bordoni peaks in copper and silver during electron irradiation at 110 K and subsequent annealing up to 300 K. Lam et al. [10] performed calculations of the properties of small vacancy and interstitial clusters for the same pair of materials. Except for tri-, tetra-, and pentavacancies, the stable configurations for small vacancy clusters were the same in both metals. The binding energies were linear functions of the number of vacancies in the cluster for defects larger than pentavacancies. The binding and migration energies for the divacancies were smaller than for the monovacancies. In turn, Shimomura [11], using electron microscopy, investigated pure silver exposed

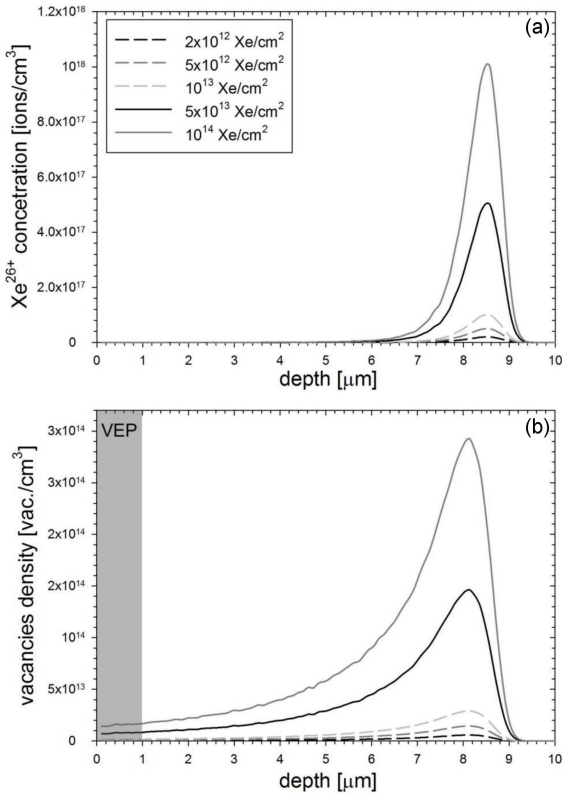

Fig. 1. SRIM/TRIM [14] calculations of ion concentration (a) and vacancies density (b) depending on the depth for silver irradiated with 167 MeV Xe^{26+} with different doses.

to irradiation with 3 MeV electrons near 1400 K. There were found interstitial loops below the III stage of annealing. Their number was constant, but the size of the loops increased with increasing dose. Defects induced in silver polycrystalline irradiated with 4 keV Ar^+ were investigated by Duarte Naia et al. [12] using a variable energy positron beam. They observed the interaction of the gas with the produced damages. Additionally, two regions were recognized. The first one was found near the surface and was occupied by vacancy-type defects involved by irradiation. The second region, deeper one, was created due to the coalescence of Ar. Deeper defects evolved there with thermal treatments and probably produced cavities. Dryzek et al. [13] recognized dislocations or vacancies associated with dislocations regardless of the dose in heavy ion implanted silver.

This paper reports experimental studies of pure silver samples exposed to irradiation with heavy Xe^{26+} ions. Implantation induces open-volume defects, the presence of which should be reflected in the PAS characteristics. The goal of this study is to obtain information about the dose dependency on changes generated by irradiation in the structure of the near-surface region. The variable energy positron beam (VEP) was used for this aim.

2. Experimental details

2.1. Sample preparation

The plates of 99.8% purity silver with dimensions $15 \times 15 \times 3$ mm^3 were annealed for 2 h at 1000°C in vacuum conditions of 10^{-5} Torr and cooled down in a closed furnace to room temperature. This approach allows one to get all samples in the same state, containing only residual defects in their structures. One sample has been saved as the reference one. Others were exposed to heavy ion irradiation. This experiment was performed using the IC-100 cyclotron operating at the Flerov Laboratory of Nuclear Reactions at Joint Institute for Nuclear Research (JINR) in Dubna, Russia. Xe^{26+} ions with energy of 167 MeV and different doses: 2×10^{12}, 5×10^{12}, 10^{13}, 5×10^{13} and 10^{14} ions/cm^2 were used. The average ion flux was 5×10^9 cm^{-2} s^{-1}. The temperature during irradiation did not exceed 80°C. According to SRIM/TRIM [14] calculations (see Fig. 1), the maximum of the Bragg peak lies at a depth of about 8.3 μm, while the thickness of the implanted layer is close to 9.2 μm. Additionally, the concentration of ions and defects increases with the dose.

2.2. VEP tests

Experiments were performed at room temperature using VEP at the Dzhelepov Laboratory of Nuclear Problems at JINR in Dubna (Russia) [15]. A continuous positron flux with a diameter of 3 mm and an energy varing from 0.1 up to 36 keV has been used. The intensity of the beam was about 10^6 e^+/s.

The thickness of the samples tested with VEP, marked by grey colour in Fig. 1b, is ca. 1 μm for this beam. It was estimated on the basis the following formula

$$\bar{z} = \frac{A\,E^n}{\rho}, \tag{1}$$

where $A = 3.66$ μg cm^{-2} keV^{-n}, $n = 1.576$, and ρ is the density equal to 10.49 g/cm^3. In this way, the near-surface region where ions slow down due to electronic energy loss processes was investigated.

The Doppler broadening (DB) spectra were measured with a high purity germanium (HPGe) detector characterized by an energy resolution (FWHM) equal to 1.2 keV for an energy of 511 keV. The analysis of the annihilation line consisted of the evaluation of the standard shape-parameters S and W. The first parameter is given as the ratio of the area below the central part of the 511 keV line to the total area below this line. This ratio increases with higher defect concentration and reveals the positron annihilation with low momentum electrons. In turn, the second parameter, representing the annihilation with core electrons, is defined as the area under the wing part of the peak to the whole area of the peak representing the fraction. Together with the S parameter, W delivers limited information about changes in defects types.

3. Results and discussion

The values of the S and W parameters measured depending on the positron incident energy have been shown in Fig. 2. On the top axis, the mean implantation depth obtained from (1) is presented. The white circles represent the reference well-annealed sample. Dark grey points of different shapes symbolise implanted specimens. Note that the S parameter decreases with energy and saturates. The sharp fall noticed at the beginning of the S parameter profiles is caused by the positron diffusion back to the surface. The flat part of the distribution means annihilation at depths far from the surface. In the case of irradiated samples, the level of saturation is higher than for the reference specimen. Additionally, it increases with the dose. This definitely points out the existence of irradiation-induced defect and increases their concentration with fluence.

In turn, completely different behaviour is noticed for the $W(E)$ distributions presented at the bottom of Fig. 2. These are reflection of the $S(E)$ profiles in terms of abscissa. For all samples, the W parameter increases and stabilizes. The presence of open-volume defects produced by irradiation occurs in a lower level of saturation. Similarly, it decreases with arising dose. The opposite tendencies between the $S(E)$ and $W(E)$ profiles are well understood. In the case of a positron trapped in defects, the fraction of annihilations with low-momentum electrons is enhanced and the number of annihilations with core electrons goes down. Referring to the definitions of both parameters (presented in the previous section), the S parameter increases and simultaneously the W parameter decreases.

Further quantitative analysis of the experimental profiles (Fig. 2) is possible on the basis of the diffusion trapping model [17]. It requires one to assume a homogeneous distribution of defects in the zone tested by VEP. Then, the code VEPFIT [18] was used to fit the dependencies shown in Fig. 2 through numerical solving of the positron diffusion equation [17]. The fitting procedure took into account one layer, density equal to 10.49 g/cm^3, and the Makhov's parameters [16] describing positron implantation as follows: $A = 3.66$ μg cm^{-2} keV^{-n}, $n = 1.576$ and $m = 1.636$. The best fits are presented by solid black lines in Fig. 2. The results are depicted in Fig. 3.

The values characterizing the saturation of the $S(E)$ profiles for the reference sample (S_{bulk}) and the irradiated (S_{def}) ones are presented in Fig. 3a. The lowest value was noticed for the unirradiated specimen. Values of S_{def} increase with fluence. There is a well-marked fast rise for low doses, followed by an increasing slowdown for higher doses. It points out a faster expansion of structural changes caused by irradiation for lower doses. It should be noticed that increasing S_{def} may reflect the development of defects concentration and their kind

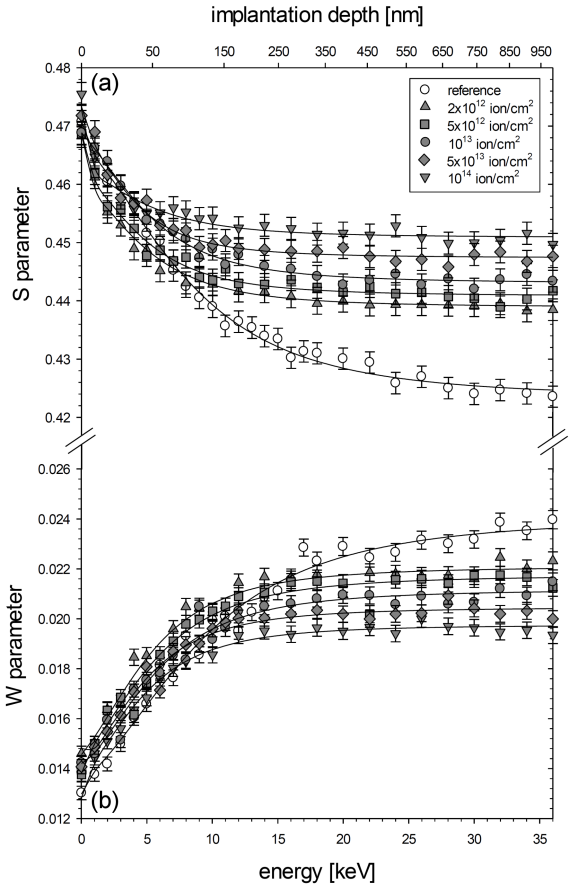

Fig. 2. The S parameter (a) and the W parameter (b) depending on the positron incident energy (bottom axis) and the mean depth (top axis) for the studied samples. Solid black lines represent the best fit from VEPFIT code [18].

as well. Similar behaviour was observed for palladium exposed to 107 MeV Kr^{17+} ions [19]. In turn, a completely different result was found for copper irradiated in the same as reported here. In that case, the dependence of S_{def} on dose (in the range 10^{12}–10^{14} ions/cm^2) was practically not observed [20].

The parameter more sensitive to detects concentration is the positron diffusion length. It is given according to the following formula [22]

$$C_v = \frac{1}{\mu\,\tau_{\mathrm{bulk}}}\left[\left(\frac{L_{\mathrm{bulk}}}{L_+}\right)^2 - 1\right], \qquad (2)$$

where μ is the trapping coefficient for a given type of defect; τ_{bulk}, L_{bulk} and L_+ are the mean positron lifetime, the diffusion length in the non-defected and defected structure, respectively. The defect concentration increases with decreasing L_+ by virtue of the above equation (2). The values of positron diffusion lengths obtaining from fitting $S(E)$ profiles (Fig. 2) are presented in Fig. 3b. The highest value 123 ± 3 nm was obtained for the unirradiated sample. This value is typical for metals [21]. Dryzek

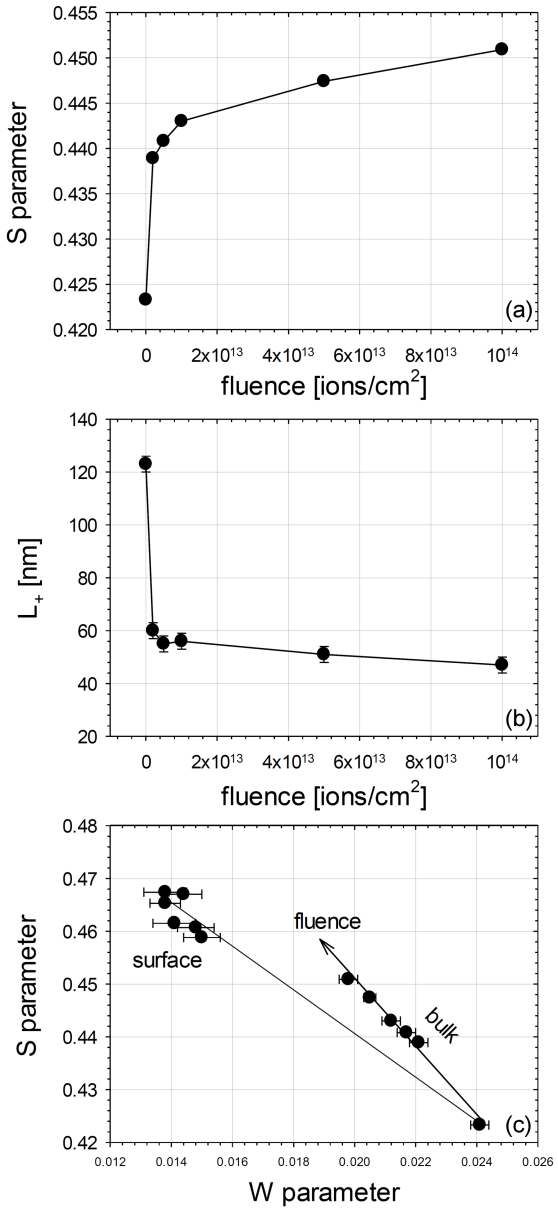

Fig. 3. Values obtained from fitting profiles shown in Fig. 2 using the VEPFIT code [18], plotted as: S parameter for saturation of $S(E)$ distributions versus dose (a), positron diffusion length depending on the dose (b) and $W(S)$ (c).

et al. [13] reported 97 ± 10 nm. However, their samples were not annealed enough because positron lifetime measurements pointed out the presence of dislocations. In turn, Duarte Naia et al. [12] found 151 nm in a non-defected sample silver. The higher value in this case can be caused by the purity of the metal, the parameters used in the fitting procedure, or the energetic range of VEP used in tests. The strong reduction of positron diffusion of the irradiated samples confirms the generation of structural defects. Moreover, shortening from 60 to 47 nm for higher fluencies delivers information about the increasing defect concentration. It should be noticed that the L_+ reduction is the smallest in the studied range of doses compared to previously reported other materials exposed to heavy ion irradiation, such as Pd [19], Cu [20] and Fe [23].

Further analysis based on the application of (2) and the obtained diffusion length cannot be provided due to the lack of knowledge about the kind of detected irradiation-induced defects. The VEP measurements with a continuous beam do not deliver any information about it. Now, (2) requests to use a trapping coefficient that is specific for the given kind of trap. Note that the positron lifetime studies of Xe^{26+} implanted silver, investigated in other contexts, only proved the existence of dislocations [24]. However, taking the assumption that only this type of defect is generated, as was done in the case of investigations reported in [22], would be an exaggeration. The measurements from [24] were performed using a positron emitted directly from a conventional positron source ^{22}Na. In experiments, positrons penetrate the total implanted thickness, where the biggest quantity of damage is located around the Bragg peak. In this way, changes visible in the range of VEP can be undetected by conventional PAS measurements. Only the defined trapping coefficient allows one to calculate the defect concentration and on this basis analyse how it depends on the dose. This is undoubtedly a disadvantage of the DB technique.

The caution against too rash assumption is supported by the behaviour visible in Fig. 3c. Values of the S parameter vs the W parameter are depicted. In fact, the $S(W)$ points represent the values obtained from fitting both the $S(E)$ and $W(E)$ profiles in Fig. 2. Information on irradiation-induced defects in studied samples can be revealed from the $S(W)$ plot. Only one kind of defect exists if all points lie on a straight line. However, in the case of the discussed results, a deviation occurs from the line connecting surface and bulk for the reference sample. Moreover, there appears another slope connected with the dose. It allows one to conclude that in studies by VEP range, irradiation fluence has an impact on the kind or size of defects, next to changes in their concentration.

4. Conclusions

Pure silver samples irradiated with 167 MeV Xe^{26+} have been studied using VEP to get the impact of irradiation doses on PAS characteristics. The existence of irradiation-induced defects has been detected. A dose dependence of all obtained features was found. In the damaged layer, the value of the S parameter for saturation of the $S(E)$ profiles increases with the fluence. Positron diffusion lengths were reduced after irradiation. Their decrease was noticed with increasing dose. However, it is smaller in comparison to other pure metals such as Pd, Cu, and Fe. Similarly, as in the case of Pd, this information allows one to conclude about

increasing the defect concentration with the dose. Probable changes in the size or kind of defects related to the applied dose were noticed. The lack of knowledge about the kind of defects could not prevent further discussion on the dependency of defects concentration on the dose. This is undoubtedly the disadvantage of the DB technique.

Acknowledgments

The authors express their gratitude to V.A. Skuratov for his technical help and assistance in ion irradiation.

References

[1] X. Hu, T. Koyanagi, Y. Katoh, B.D. Wirth, *Phys. Rev. B* **95**, 104103 (2017).

[2] M.N. Mirzayev, B.A. Abdurakhimov, E. Demir et al., *Physica B: Condensed Matter* **611**, 412842 (2021).

[3] R. Laptev, L. Svyatkin, D. Krotkevich, E. Stepanova, N. Pushilina, A. Lomygin, S. Ognev, K. Siemek, V. Uglov, *Metals* **11**, 627 (2021).

[4] T. Iwai, H. Tsuchida, M. Awano, *J. Nucl. Mater.* **367–370**, 372 (2007).

[5] I. Martina, R. Wiesinger, D. Jembrih-Simbürger, M. Schreiner, *e-PS* **9**, 1 (2012).

[6] D. Jembrih-Simbürger, C. Neelmeijer, O. Schalm, P. Fredrick, M. Schreiner, K. De Vis, M. Mäder, D. Schryvers, J. Caen, *J. Anal. At. Spectrom.* **17**, 321 (2002).

[7] M.L. Jenkins, *Philos. Mag.* **29**, 813 (2006).

[8] M.M. Ahmad, E.A. Abdel-Wahab, A.A. El-Maaref, M. Rawway, E.R. Shaaban, *SpringerPlus* **3**, 443 (2014).

[9] P. Lauzier, C. Girard, A. Minier, *J. Phys. Colloq.* **42**, 247 (1981).

[10] N.Q. Lam, N.V. Doan, L. Dagens, *J. Phys. F Met. Phys.* **15**, 799 (1985).

[11] Y. Shimomura, *J. Appl. Phys.* **41**, 749 (1970).

[12] M. Duarte Naia, P.M. Gordo, O.M.N.D. Teodoro, A.P. de Lima, A.M.C. Moutinho, R.S. Brusa, *Mater. Sci. Forum* **514–516**, 1608 (2006).

[13] J. Dryzek, P. Horodek, V.S. Skuratov, *Acta Phys. Pol. A* **135**, 1585 (2017).

[14] J.F. Ziegler, *The Stopping and Range of Ions in Solids*, 2nd ed., Academic Press, New York 1988.

[15] P. Horodek, A.G. Kobets, I.N. Meshkov, A.A. Sidorin, O.S. Orlov, *Nukleonika* **60**, 725 (2015).

[16] J. Dryzek, P. Horodek, *Nucl. Instrum. Methods Phys. Res. B* **266**, 4000 (2008).

[17] T.E.M. Staab R. Krause-Rehberg, B. Kieback, *J. Mater. Sci.* **34**, 3833 (1999).

[18] A. Van Veen, H. Schut, M. Clement, A. Kruseman, M.R. Ijpma, J.M.M. De Nijs, *Appl. Surf. Sci.* **85**, 216 (1995).

[19] P. Horodek, V.A. Skuratov, *Surf. Coat. Technol.* **296**, 65 (2016).

[20] P. Horodek, J. Dryzek, V.A. Skuratov, *Vacuum* **138**, 15 (2017).

[21] P.J. Schultz, K.G. Lynn, *Rev. Mod. Phys.* **60**, 701 (1988).

[22] W. Qiang-mao, S. Guo-gang, W. Rongshan, D. Hui, P. Xiao, Z. Qia, L. Jing, *Nucl. Instrum. Methods Phys. Res. B* **287**, 148 (2012).

[23] P. Horodek, J. Dryzek, V.A. Skuratov, *Rad. Phys. Chem.* **122**, 60 (2016).

[24] J. Dryzek, P. Horodek, M. Dryzek, *Appl. Phys. A* **124**, 451 (2018).